Journal of Inflammation Research

Dovepress
Taylor & Francis Group

Open Access Full Text Article

ORIGINAL RESEARCH

SIRT1 Enhancement is Required for the Induction of Anti-Inflammatory Effect of Micheliolide in Carbon Tetrachloride Induced Liver Fibrosis in Mice

Chengye Jin[1,*], Aoqing Jiang[1,*], Jieming Chang[1], Yirong Hu[1], Yichen Wang[1], Rui Zhao[1], Jingwei Shi[2], Hongyan Wu[3], Zhongliang Han[1], Zhaoguo Liu[1]

[1]School of Pharmacy, Nantong University, Nantong, Jiangsu, People's Republic of China; [2]School of Medicine, Nantong University, Nantong, Jiangsu, People's Republic of China; [3]Institute of Biomedical Technology, Jiangsu Medical College, Yancheng, Jiangsu, People's Republic of China

*These authors contributed equally to this work

Correspondence: Zhaoguo Liu, School of Pharmacy, Nantong University, Nantong, Jiangsu, People's Republic of China, Tel +86 513 8505 1726, Fax +86 513 8505 1728, Email lzg871014@ntu.edu.cn

Purpose: Micheliolide (MCL), a guaianolide sesquiterpene lactone isolated from *Michelia compressa* and *Michelia champaca*, exhibits diverse pharmacological activities, with particularly potent hepatoprotective effects. However, research on its effects against liver fibrosis and underlying mechanisms remains limited. This study aimed to investigate the protective role of MCL in carbon tetrachloride (CCl_4)-induced liver fibrosis in mice and elucidate the potential mechanisms, with a focus on the regulation of Sirtuin 1 (SIRT1).

Methods: Liver fibrosis model was established in mice via intraperitoneal (i.p.) injections of 10% CCl_4. Serum biochemical indicators and liver fibrosis biomarkers were investigated. Liver collagen deposition was assessed by Masson and Sirus red staining. Protein and inflammatory cytokine expression levels were assessed using qRT-PCR, Western blot, ELISA, Immunohistochemistry staining, and Tissue immunofluorescence assays.

Results: MCL attenuated CCl_4-induced liver injury and restored hepatic function in mice. Mechanistically, MCL reduced liver collagen deposition, downregulated the protein expression of α-smooth muscle actin (α-SMA) and fibronectin in liver tissues, and decreased serological markers of liver fibrosis. Additionally, MCL suppressed the serum levels of pro-inflammatory cytokines interleukin-1β (IL-1β), IL-6, tumor necrosis factor-α (TNF-α), and monocyte chemoattractant protein-1 (MCP-1) while increasing IL-10 levels. Notably, CCl_4 administration caused a significant reduction in SIRT1 protein and mRNA expression, which was markedly reversed by MCL treatment. The selective SIRT1 inhibitor EX-527 abrogated both the anti-liver injury and anti-fibrotic effects of MCL. Moreover, EX-527 also attenuated MCL-mediated suppression of liver inflammation in CCl_4-induced fibrotic mice.

Conclusion: MCL mitigates CCl_4-induced liver injury and fibrosis by activating SIRT1 to suppress liver inflammation in mice. These findings uncover a novel molecular mechanism for the anti-liver fibrotic activity of MCL and highlight its potential as a therapeutic candidate for liver fibrosis.

Keywords: micheliolide, carbon tetrachloride, liver fibrosis, inflammation, SIRT1

Introduction

Liver fibrosis is defined as a dysregulated wound-healing process, primarily characterized by the excessive accumulation of extracellular matrix (ECM).[1] Liver inflammation is tightly associated with the progression of liver fibrosis and is widely recognized as a pivotal initiating factor that drives the onset of this fibrotic process.[2] Studies have demonstrated that the liver mounts an inflammatory response upon exposure to diverse detrimental stimuli, including viral infections, drug-induced injury, alcohol-mediated toxicity, and autoimmune disorders. This inflammatory cascade causes significant damage to hepatocytes, ultimately leading to cell necrosis.[3] Concurrently, such cellular stress activates hepatic stellate cells (HSCs), which subsequently undergo phenotypic transformation into myofibroblasts. These activated myofibroblasts then synthesize and secrete excessive amounts of ECM components, such as collagen and fibronectin. As these

Received: 7 August 2025
Accepted: 12 November 2025
Published: 19 November 2025

ECM proteins accumulate excessively within the liver parenchyma, progressive tissue remodeling occurs, ultimately resulting in the development of liver fibrosis.[4] Therefore, effective inhibition of the hepatic inflammatory response represents a promising strategy for the management of liver fibrosis.

SIRT1, a nicotinamide adenine dinucleotide (NAD+)-dependent histone deacetylase, belongs to the silent information regulator 2 (SIR2) family.[5] It exerts multifaceted roles in physiological processes, primarily including the regulation of gene expression, modulation of energy metabolism, and maintenance of intracellular homeostasis. Additionally, the SIRT1 protein is widely involved in the pathological progression of various other diseases, such as neurodegenerative diseases, cardiovascular diseases, atherosclerosis, and tumors.[6,7] In liver-related disorders, SIRT1 participates extensively in the development of diverse liver diseases and has been recognized as a key target for disease intervention.[8] It also plays a pivotal role in the pathogenesis of liver fibrosis; activation of SIRT1 can effectively suppress the activation of hepatic stellate cells (HSCs), thereby contributing to the efficient control of liver fibrosis progression.[9] Notably, studies have demonstrated that SIRT1 can effectively inhibit hepatic inflammation by deacetylating NF-κB p65,[10] which highlights a regulatory relationship between SIRT1 and liver inflammation.

Micheliolide (MCL) is a guaianolide-type sesquiterpene lactone. Its chemical structure is shown in Figure 1. MCL has been isolated from *Michelia compressa* and *Michelia champaca*.[11] Previous studies have found that MCL has a wide range of pharmacological effects, such as anti-osteoporotic, anti-neuroinflammatory, anti-acute lung injury, ameliorating diabetic kidney disease, and anti-tumor activities.[12,13] Moreover, MCL also exhibits certain hepatoprotective effects, which can effectively alleviate hepatic steatosis and inhibit liver cancer.[14,15] Notably, a recent study has demonstrated that MCL exhibits anti-fibrotic effects in the liver.[16] However, the role of SIRT1 protein in MCL-mediated regulation of liver fibrosis has not yet been reported. In this study, we used a CCl_4-induced liver fibrosis model in mice to assess the anti-fibrotic effect of MCL. Additionally, we used the SIRT1 selective inhibitor EX-527 to clarify the prospective function of SIRT1 in the MCL-induced anti-fibrotic effect.

Materials and Methods

Chemicals and Reagents

Mecheliolide (PS021107, ≥ 98%) was bought from Chengdu PUSH Bio-Technology Co., Ltd (Chengdu, China). CCl_4 (CAS. NO. 56-23-5) was purchased from Shanghai Xilong Chemical Co., Ltd (Shanghai, China). Colchicine (Cat. No. ST1173) and Corn oil (Cat. No. ST1177) were obtained from Beyotime (Shanghai, China). Hyaluronic acid (HA) (cby24074) ELISA kit, Procollagen Type III (PC-III) (cby24660) ELISA kit, and mouse monocyte chemotactic protein 1 (MCP-1) ELISA kit (cby23209) were acquired from Nanjing Herb Source Bio-Technology Co., Ltd (Nanjing, China).

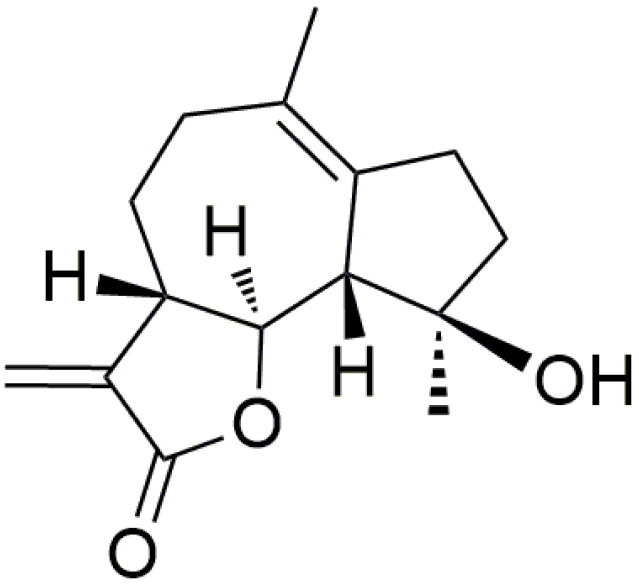

Figure 1 Chemical structure of micheliolide (MCL). Chemical Formula of micheliolide is $C_{15}H_{20}O_3$. Molecular weight of micheliolide is 248.32kDa.

Hydroxyproline content assay kit (Cat# BC0250) was bought from Beijing Solarbio Science & Technology Co., Ltd (Beijing, China). Mouse IL-1β ELISA kit (EMC001b), mouse IL-6 ELISA kit (EMC004) and mouse tumor necrosis factor-α (TNF-α) (EMC102a) were obtained from NeoBioscience Technology Co., Ltd (Shenzhen, China). Mouse IL-10 ELISA kit (YT-0176M2) was bought from Jiangsu Yutong Biotechnology Co., Ltd (Yancheng, China). Smooth muscle actin (α-SMA) (14395-1-AP), Collagen I (14695-1-AP) and Fibronectin (15613-1-AP) antibodies were purchased from Proteintech (Chicago, USA). Sirtuin 1 (SIRT1) (BF0189) antibody was purchased from Affinity (Changzhou, China). Selisistat (EX-527) (Cat# S1541) was bought from Selleck (Houston, USA). PEG300 (Cat # HY-Y0873) was acquired from MedChemExpress (New Jersey, USA). The other chemicals/reagents were of analytical quality or higher grade.

Animal Experimental Protocol

C57BL/6JNifdc male mice (4-week-old, 20–22 g) were procured from Nantong Jingqi Biotechnology Co., Ltd. (Nantong, China). Experimental protocols were approved by the Institutional Animal Care and Use Committee of Nantong University (Approval No. S20200907-306) and conducted in strict accordance with the National Institutes of Health (USA) guidelines for humane animal care. The liver fibrosis model was established in accordance with the previously reported protocol.[17] Briefly, mice received intraperitoneal (i.p.) injections of 10% CCl_4 (1:9 dilution in corn oil, v/v) three times weekly for eight consecutive weeks, while control mice received an equivalent volume of corn oil via i.p. injection. From weeks 5 to 8, mice were gavaged daily with MCL dissolved in corn oil at dosages of 15 or 60 mg/kg. All mice were euthanized 12 hours after the final treatment. Blood was collected via retro-orbital plexus puncture, and serum was separated by centrifugation at 3000 rpm for 10 minutes at 4°C. Livers were immediately excised for subsequent analyses.

For liver fibrosis experiments with EX-527 treatment: C57BL/6JNifdc male mice (4-week-old, 20–22 g) were obtained from Nantong Jingqi Biotechnology Co., Ltd. (Nantong, China). Fifty mice were randomly allocated into five groups (10 mice per group): Control, CCl_4, CCl_4+EX-527 (10 mg/kg), CCl_4+MCL (60 mg/kg), and CCl_4+EX-527 (10 mg/kg)+MCL (60 mg/kg). The fibrosis model was induced as described above, with mice receiving 10% CCl_4 (1:9 in corn oil, v/v) via i.p. injection three times weekly for eight weeks. From weeks 5 to 8, the SIRT1 selective inhibitor EX-527 (10 mg/kg) was administered by i.p. injection every other day, while MCL (60 mg/kg) was delivered by daily intragastric gavage. Mice were euthanized 12 hours after the final treatment, and blood/serum collection followed the same protocol as above. Livers were promptly dissected for subsequent analyses.

Histopathological and Collagen Deposition Examination

Livers were fixed in 10% formalin, paraffin-embedded, sectioned at 5 μm thickness, and stained with hematoxylin and eosin (H&E), Masson's trichrome, and Picro-Sirius red using standard protocols to assess pathological injury and collagen deposition. All staining procedures followed established methodologies. Photomicrographs were captured in a blinded manner across random fields of view, and representative images of liver sections are presented.

Biochemical Index Detection

The serum concentrations of alkaline phosphatase (ALP), alanine aminotransferase (ALT), aspartate aminotransferase (AST), lactic dehydrogenase (LDH), and total bilirubin were quantified using commercial assay kits, with all procedures strictly adhering to the manufacturers' protocols. Each experiment was independently conducted in triplicate to ensure reproducibility.

Enzyme-Linked Immunosorbent Assay (ELISA)

Serum levels of hyaluronic acid (HA), procollagen type III (PC-III), laminin (LN), interleukin-1β (IL-1β), IL-6, tumor necrosis factor-α (TNF-α), monocyte chemotactic protein 1 (MCP-1), and IL-10 were quantified using ELISA kits, with all procedures strictly following the manufacturers' protocols. Additionally, hepatic IL-10 levels in mouse livers were assayed by ELISA according to established methods. Each experiment was independently repeated in triplicate to ensure reproducibility.

Immunohistochemistry Staining

Immunohistochemical analyses were conducted according to the previous study.[18] Briefly, paraffin-embedded liver tissues were sectioned at 4 μm thickness, followed by deparaffinization and serial dehydration in ethanol solutions (75%, 85%, 95%, 100%). Antigen retrieval was performed using EDTA buffer. Liver sections were then incubated with primary antibody against Collagen I (1:200, proteintech), α-SMA (1:3000, proteintech) and Fibronectin (1:100, proteintech) at 4°C overnight. After washing, sections were treated with secondary antibody at room temperature for 30 minutes, followed by Diaminobenzidine (DAB) staining and hematoxylin counterstaining. Positive areas were identified by brownish-yellow pigmentation. Immunohistochemical analyses were conducted using Image-Pro Plus software 6.0.

Tissue Immunofluorescence

Following deparaffinization, 5-μm-thick liver tissue sections were blocked with 1% bovine serum albumin and incubated overnight at 4°C with IL-1β, SIRT1, and IL-6 antibodies. After three PBS washes, the sections were incubated with secondary antibodies at room temperature for 1 hour. Negative controls consisted of sections incubated with secondary antibodies alone. Images were captured in a single plane using an MRC 1024 laser confocal microscope (Bio-Rad Laboratories).

Western Blot Analysis

Fifty-microgram protein samples were separated by 10% SDS-PAGE, transferred to PVDF membranes, and blocked with 5% BSA. Membranes were incubated with primary antibodies at 4°C overnight, followed by secondary antibodies (1:5000) for 90 minutes. Blots were visualized using an ECL chemiluminescence kit (Beyotime Biotechnology, Shanghai, China). GAPDH antibody was used to verify equal protein loading. Relative protein levels were analyzed by ImageJ software (National Institutes of Health, Bethesda, MD, USA). Representative blots were derived from triplicate experiments.

Isolation of RNA and Real-Time PCR

Total RNA was isolated from liver tissues using the total RNA fast isolation kit (BioTeke, China), and a commercially available kit was then employed to synthesize cDNA as per provided protocols. Gene expressions were measured by performing qPCR with CFX Connect™ Real-Time PCR System (Bio-Rad, USA), and relative mRNA expression was quantified with the comparative cycle threshold (Ct) method and expressed as $2^{-\Delta\Delta Ct}$ method with normalization against GAPDH mRNA. *α-SMA*: (forward) 5′-CCACCATCTGCCTG AAATCC-3′, (reverse) 5′-GCTTCTTGTCC AGCCTCCTC-3′; *SIRT1*: (forward) 5′-AGTTCCAGCCGTCTCTGTGT-3′, (reverse) 5′-CTCCACGAACAGCTTCACAA-3′; GAPDH: (forward) 5′-GCACAGTCAAGGCCGAGAA TGG-3′, (reverse) 5′-GGTGGCAGTGATGGCATGGAC-3′.

Statistical Analyses

All values are presented as mean ± SD. Statistical analysis was performed using Student's *t*-test and one-way ANOVA by GraphPad Prism 5 for Windows. Values of $P< 0.05$ were considered statistically significant.

Results

MCL Alleviated CCl_4-Induced Liver Injury in Mice

The protective efficacy of MCL against CCl_4-induced hepatic injury was systematically evaluated. Morphological analysis revealed that MCL significantly ameliorated histological alterations in liver tissues of CCl_4-treated mice (Figure 2A). Macroscopic examination showed that CCl_4 induction resulted in rough, dull liver surfaces in mice, whereas MCL treatment restored tissue smoothness and lustre (Figure 2B). Histopathological assessment further demonstrated that MCL effectively mitigated fibrotic septum formation, hepatocellular necrosis, steatosis, and vacuolation, as evidenced by reduced pathological lesions in liver tissues of CCl_4-exposed mice (Figure 2B). Biochemically, MCL significantly attenuated the CCl_4-induced elevation of serum ALP, ALT, AST, LDH, and total bilirubin levels (Figure 2C–G). Colchicine, served as a positive control drug, also demonstrated the capacity to ameliorate CCl_4-induced liver injury (Figure 2A–G). Additionally, CCl_4 administration significantly increased the liver/body weight ratio in mice, and MCL treatment was able

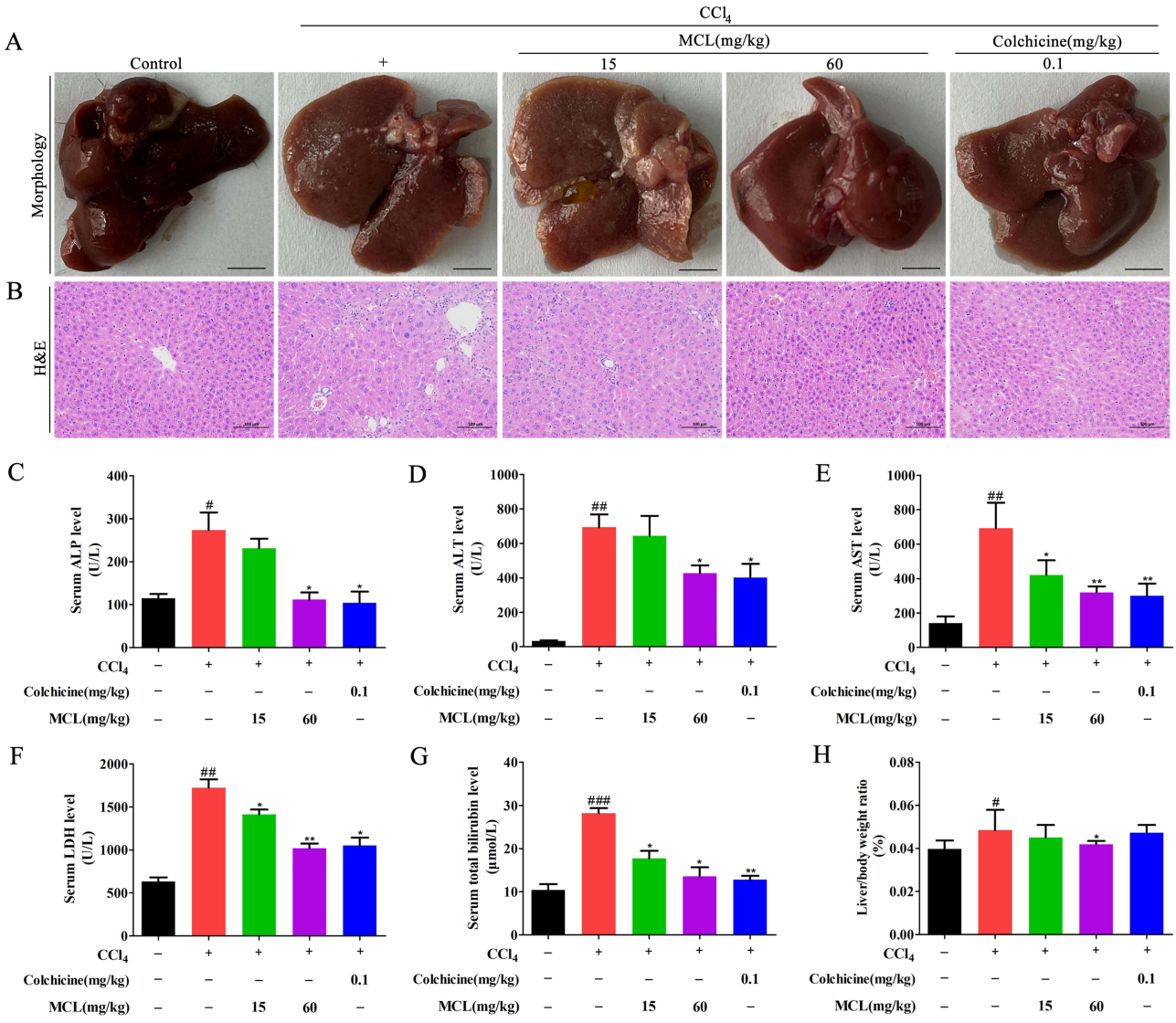

Figure 2 Effect of MCL on liver injury in CCl_4-treated mouse livers. (**A**) The morphology changes of liver in mice (scale bar: 0.5 cm). (**B**) Liver sections were stained with H&E for histological examination. Red arrows indicate liver pathological damage. Representative photographs are shown (200 × magnification, scale bar: 100 μm). (**C–G**) Detection of sera levels of ALP, ALT, AST, LDH and total bilirubin by assay kits, respectively. (**H**) The liver/body weight ratio (%). Data are expressed as mean ± SD (n= 3 of 10 mice). $^{\#}p<0.05$, $^{\#\#}p< 0.01$ and $^{\#\#\#}p< 0.001$ vs the control group; $^{*}p< 0.05$ and $^{**}p< 0.01$ vs the CCl_4 alone group.

to normalize this CCl_4-induced disturbance in the liver/body weight ratio (Figure 2H). It is worth noting that HE staining results revealed no pathological changes in mouse organs following the administration of MCL alone compared to the control group (Figure S1A in supplementary materials). Additionally, kit-based assays showed that MCL administration alone had no significant impact on serum ALP, ALT, or AST levels in mice relative to the control group (Figure S1B-D in supplementary materials), highlighting that MCL does not induce systemic toxicity in mice. Collectively, these findings indicate that MCL potently alleviates CCl_4-induced liver injury in mice.

MCL Decreased CCl_4-Induced Collagen Deposition and Inhibited CCl_4-Induced Liver Fibrosis in Mice

CCl_4 exposure induces hepatic injury and promotes excessive collagen deposition in liver tissue, thereby contributing to the development of liver fibrosis.[1] To investigate the effect of MCL on CCl_4-induced collagen accumulation, Masson's trichrome and Sirius red staining were employed to visualize collagen deposition. CCl_4 administration significantly enhanced collagen deposition in murine liver tissues, whereas MCL treatment potently reduced this fibrotic response

https://doi.org/10.2147/JIR.S559076

(Figure 3A–E). Additionally, CCl_4 exposure induced significant upregulation of Collagen I protein expression in mouse liver tissues, whereas MCL treatment potently downregulated Collagen I expression (Figure 3C and F). The anti-fibrotic effect of MCL against CCl_4-induced liver fibrosis was further investigated. MCL significantly downregulated the protein expression of α-SMA and fibronectin, two established marker proteins of liver fibrosis, in mouse liver tissues (Figure 4A–C). Furthermore, MCL remarkably reduced the serum levels of hyaluronic acid (HA), type III procollagen (PC-III), and laminin (LN), three well-recognized serological markers of liver fibrosis (Figure 4D–F). Besides, Western blot and RT-PCR analyses demonstrated that MCL potently inhibited both the protein and mRNA expression of α-SMA in murine liver tissues (Figure 4G–I). Taken together, these findings indicated that MCL effectively reduced CCl_4-induced collagen deposition and suppressed the progression of liver fibrosis in mice.

MCL Suppressed CCl_4-Induced Liver Inflammation in Mice

Inflammation is widely recognized as the initiating factor in the pathogenesis of hepatic fibrosis, and the inhibition of inflammatory responses can effectively impede the progression of hepatic fibrosis.[19] Therefore, we further investigation into the effect of MCL on CCl_4-induced liver inflammation in mice. CCl_4 induction led to a significant elevation in serum levels of pro-inflammatory cytokines IL-1β, IL-6, TNF-α, and MCP-1 (Figure 5A–D), while reducing the levels of anti-inflammatory cytokine IL-10 (Figure 5E and F) in both serum and liver tissues of mice. Conversely, MCL administration effectively decreased

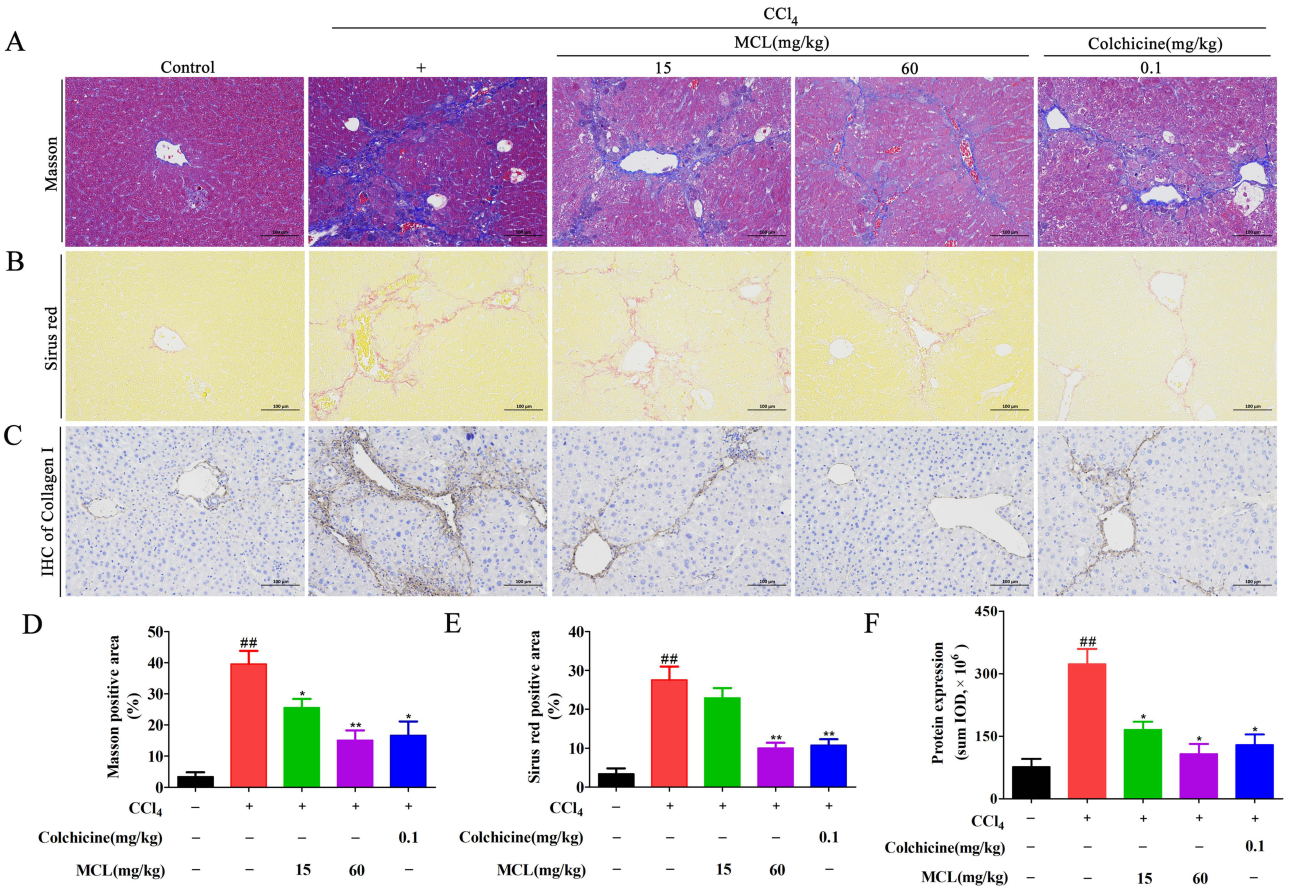

Figure 3 Effect of MCL on collagen deposition in CCl_4-treated mouse livers. (**A**) Liver sections were stained with Masson reagent. Representative photographs are shown (200 × magnification, scale bar: 100 μm). (**B**) Liver sections were stained with Sirius red reagent. Representative photographs are shown (200 × magnification, scale bar: 100 μm). (**C**) Examination of the protein expression of Collagen I by immunohistochemical staining in mouse liver tissues. Representative photographs are shown (200 × magnification, scale bar: 100 μm). (**D**) Quantified the positive area of Masson staining. (**E**) Quantified the positive area of Sirius red staining. (**F**) Quantified immunohistochemical results of liver proteins. Data are expressed as mean ± SD (n= 3 of 10 mice). $^{\#\#}p< 0.01$ vs the control group; *p< 0.05, **p< 0.01 vs the CCl_4 alone group.

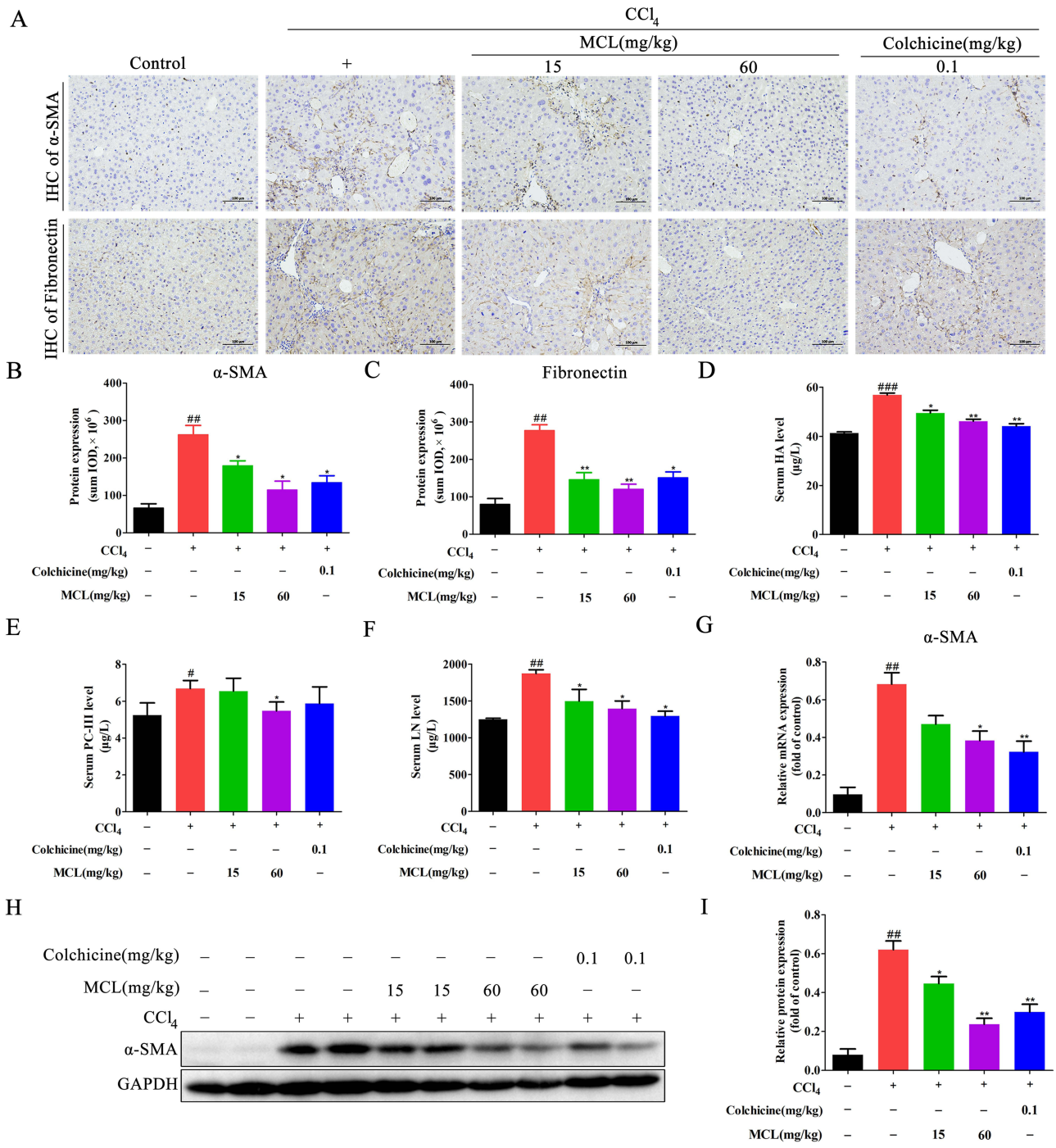

Figure 4 Effect of MCL on expression of liver fibrosis markers in CCl_4-treated mouse livers. (**A**) Examination of the protein expression of α-SMA and Fibronectin by immunohistochemical staining in mouse liver tissues. Representative photographs are shown (200 × magnification, scale bar: 100 μm). (**B** and **C**) Quantified immunohistochemical results of liver proteins. (**D–F**) Examination of sera levels of HA, PC-III and LN by assay kits in CCl_4-treated mouse mice, respectively. (**G**) Detection of the mRNA expression of α-SMA in CCl_4-treated mouse livers. (**H**) Examination of the protein expression of α-SMA by Western blot in CCl_4-treated mouse livers. (**I**) Quantified Western blot results of liver proteins. Data are expressed as mean ± SD (n= 3 of 12 mice). $^{\#}p< 0.05$, $^{\#\#}p< 0.01$ and $^{\#\#\#}p< 0.001$ vs the control group; $^{*}p < 0.05$ and $^{**}p < 0.01$ vs the CCl_4 alone group.

the levels of pro-inflammatory cytokines and restored the level of anti-inflammatory cytokine. Moreover, Immunofluorescence analysis further demonstrated that MCL significantly suppressed IL-1β protein expression in liver tissues of fibrotic mice (Figure 5G). Altogether, the above experimental results indicated that MCL inhibited CCl_4-induced liver inflammation in mice.

https://doi.org/10.2147/JIR.S559076

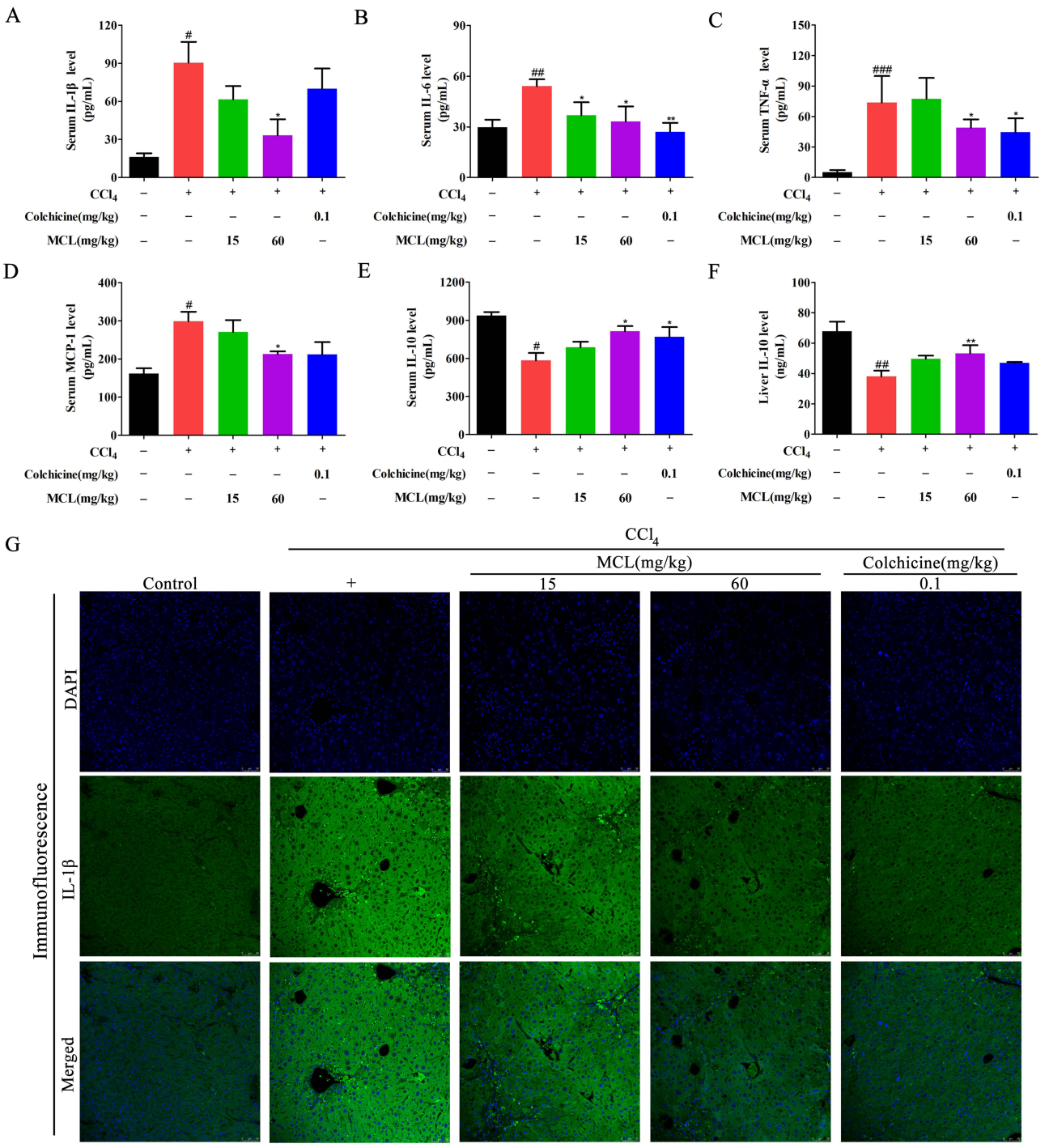

Figure 5 Effect of MCL on liver inflammation in CCl_4-treated mouse livers. (**A–E**) Examination of sera levels of IL-1β, IL-6, TNF-α, MCP-1 and IL-10 by assay kits, respectively. (**F**) Examination of IL-10 level in in CCl_4-treated mouse livers. (**G**) Immunofluorescence assay was performed to detect the protein expression of IL-1β in mouse liver tissues. Data are expressed as mean ± SD (n= 3 of 10 mice). $^{\#}p < 0.05$, $^{\#\#}p < 0.01$ and $^{\#\#\#}p < 0.001$ vs the control group; $^{*}p < 0.05$ and $^{**}p < 0.01$ vs the CCl_4 alone group.

MCL Enhanced SIRT1 Expression in CCl_4-Induced Fibrotic Livers of Mice

Previous studies have established that SIRT1 is intricately linked to the pathogenesis of liver fibrosis and has been identified as a pivotal target for therapeutic intervention in liver fibrosis.[20] Therefore, we wondered whether the anti-liver fibrosis effect of MCL is linked to the regulation of SIRT1 protein. To address this question, we first investigated the effect of MCL on SIRT1 protein expression in the pathological milieu of liver fibrosis. Western blot and RT-PCR

analyses demonstrated that CCl_4 induction significantly downregulated SIRT1 protein and mRNA expression in liver tissues of mice compared with the control group. In contrast, MCL treatment potently reversed this downregulation, restoring SIRT1 expression at both the transcriptional and translational levels (Figure 6A–C). Results from both immunofluorescence and immunohistochemical analyses also confirmed that MCL significantly enhanced SIRT1 protein expression in liver tissues of mice (Figure 6D–G). Interestingly, the positive control drug colchicine failed to upregulate SIRT1 protein expression in mouse liver tissues (Figure 6A–F). Collectively, MCL enhanced SIRT1 expression in CCl_4-induced fibrotic livers of mice.

Pharmacological Blockade of SIRT1 Abrogated the Hepatoprotective Efficacy of MCL Against CCl_4-Induced Liver Injury in Mice

To further elucidate the role of SIRT1 in MCL-mediated regulation of CCl_4-induced hepatic fibrosis, we employed the selective SIRT1 inhibitor EX-527 to assess the impact of SIRT1 inhibition on the anti-fibrotic activity of MCL. Firstly, the protein and mRNA expression of SIRT1 were detected to confirm the efficacy of EX-527. Compared with the control group, treatment with EX-527 alone could reduce the protein and mRNA expression of SIRT1 in mouse liver tissue (Figure 7A–C), demonstrating the effectiveness of EX-527. In comparison with the control (CCl_4) group, EX-527 monotherapy elicited no significant impact on the morphological of mouse liver tissues. Treatment with MCL restored the lustrous and smooth hepatic surface, while EX-527 cotreatment markedly attenuated the restorative effects of MCL described above (Figure 7D). Furthermore, monotherapy with EX-527 exerted no significant effect on pathological lesions in mouse liver tissues, whereas MCL treatment markedly ameliorated CCl_4-induced histopathological damage, however, SIRT1 inhibition attenuated the

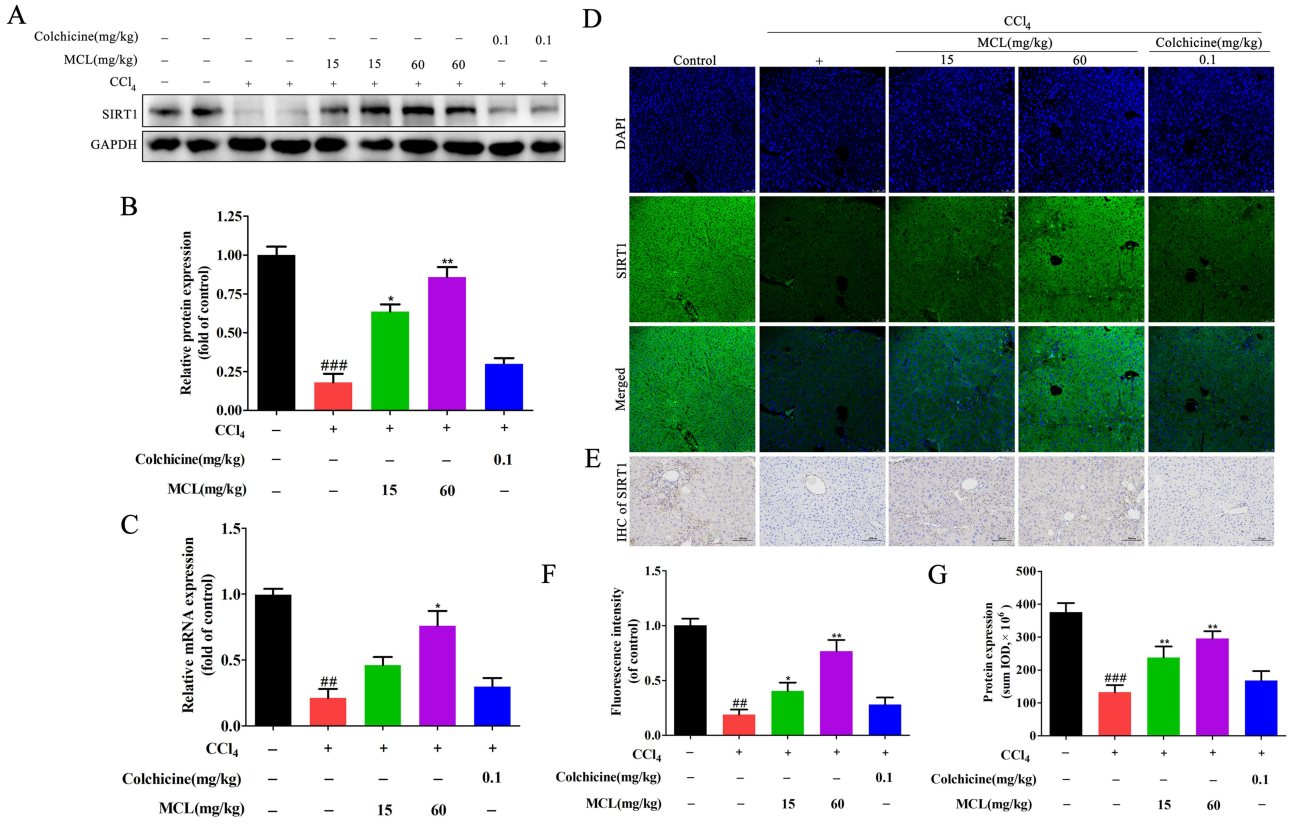

Figure 6 Effect of MCL on expression of SIRT1 in CCl_4-treated mouse livers. (**A**) Examination of the protein expression of SIRT1 by Western blot in CCl_4-treated mouse livers (n=3). (**B**) Quantified Western blot results of liver protein. (**C**) The mRNA expression of SIRT1 in CCl_4-treated mouse livers was determined by RT-PCR, respectively. (**D**) Immunofluorescence assay was performed to detect the protein expression of SIRT1 in mouse liver tissues. (**E**) Examination of the protein expression of SIRT1 by immunohistochemical staining in mouse liver tissues. Representative photographs are shown (200 × magnification, scale bar: 100 μm). (**F**) Quantified immunofluorescence results of liver proteins. (**G**) Quantified immunohistochemical results of liver proteins. Data are expressed as mean ± SD (n = 3 of 10 mice). $^{\#\#}p < 0.01$ and $^{\#\#\#}p < 0.001$ vs the control group; $^{*}p < 0.05$ and $^{**}p < 0.01$ vs the APAP-treated alone group.

https://doi.org/10.2147/JIR.S559076

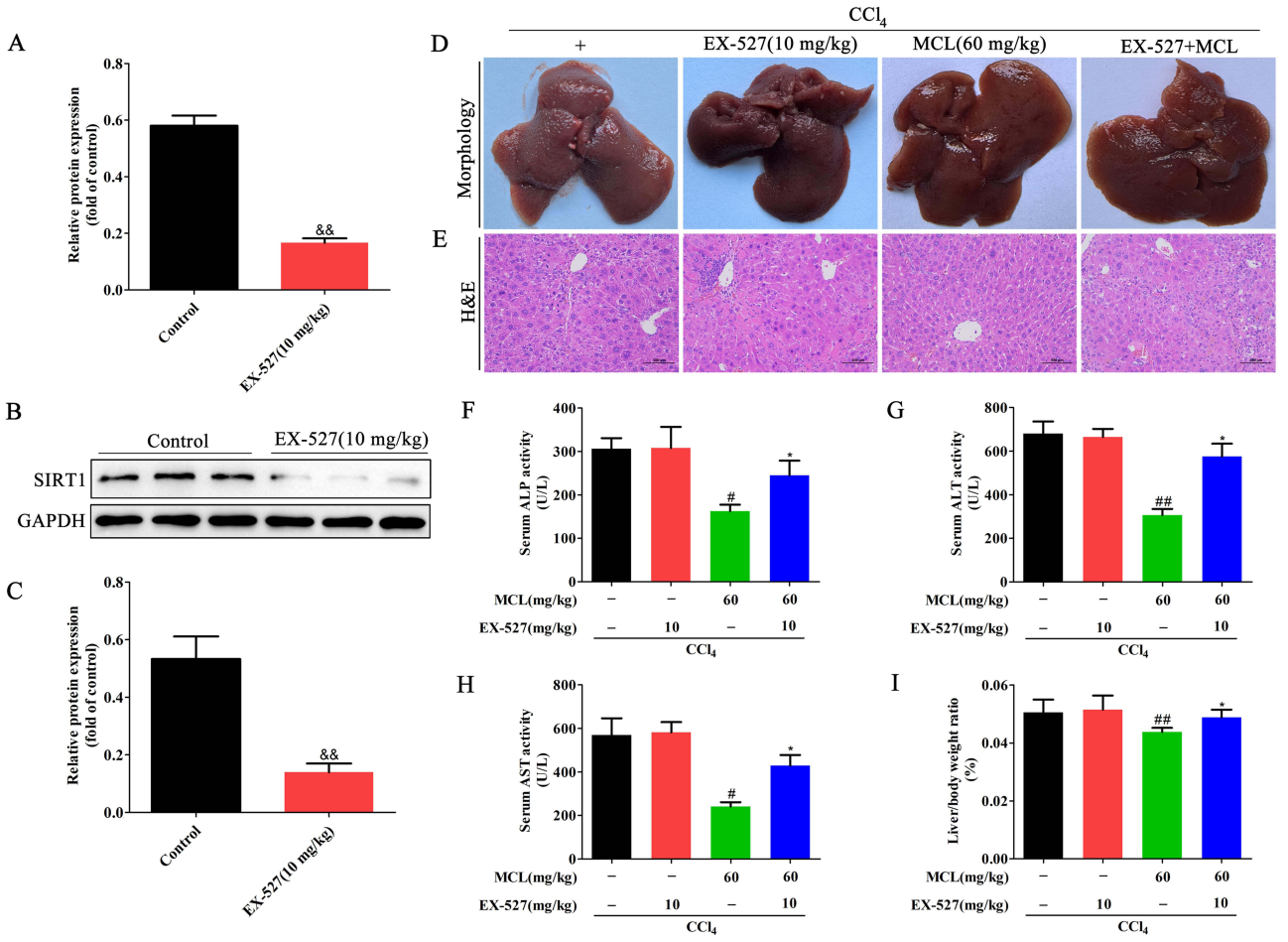

Figure 7 Effect of EX-527 (SIRT1 selective inhibitor) on liver injury regulated by MCL in CCl_4-treated mouse livers. (**A**) Examination of the mRNA expression of SIRT1 by RT-PCR in mouse liver. (**B**) Examination of the protein expression of SIRT1 by Western blot in mouse liver. (**C**) Quantified Western blot results of liver proteins. (**D**) The morphology changes of liver in mice (scale bar: 0.5 cm). (**E**) Liver sections were stained with H&E for histological examination. Representative photographs are shown (200 × magnification, scale bar: 100 μm). (**F–H**) Detection of sera levels of ALP, ALT, and AST by assay kits, respectively. (**I**) The liver/body weight ratio (%). Data are expressed as mean ± SD (n = 3 of 10 mice). $^{\&\&}p < 0.01$ vs the Control group; $^{\#}p < 0.05$ and $^{\#\#}p < 0.01$ vs the CCl_4 alone group; $^{*}p < 0.05$ vs the MCL (60 mg/kg) group.

protective efficacy of MCL against CCl_4-induced liver injury in mice (Figure 7E). Additionally, MCL treatment significantly reduced serum levels of ALP, ALT, and AST (Figure 7F–H) and decreased the liver/body weight ratio (Figure 7I) in mice, effects that were evidently abrogated by EX-527 cotreatment. Collectively, these findings demonstrate that SIRT1 inhibition abrogates the hepatoprotective efficacy of MCL against CCl_4-induced liver injury in mice.

Inhibition of SIRT1 Abolished the Anti-Fibrotic Efficacy of MCL in CCl_4-Induced Fibrotic Mice

We further investigated the effect of SIRT1 inhibition on MCL-mediated anti-fibrotic effect in mice. In comparison with the CCl_4 control group, monotherapy with EX-527 exerted no significant effect on collagen deposition in mouse liver tissues. MCL treatment markedly reduced collagen deposition, whereas cotreatment with EX-527 significantly attenuated the inhibitory effect of MCL against CCl_4-induced collagen accumulation (Figure 8A–D). Besides, hydroxyproline kit assay demonstrated that EX-527 treatment significantly attenuated the capacity of MCL to reduce serum hydroxyproline levels in mice (Figure 8E). In addition, MCL decreased the serum levels of HA and PC-III, however, were abolished by cotreatment with EX-527 (Figure 8F and G). Moreover, MCL inhibited the protein expression of α-SMA in CCl_4-induced fibrotic livers of mice, an effect also attenuated by EX-527 (Figure 8H and I). Taken together, pharmacological blockade of SIRT1 abrogated the anti-fibrotic efficacy of MCL in CCl_4-induced fibrotic mice.

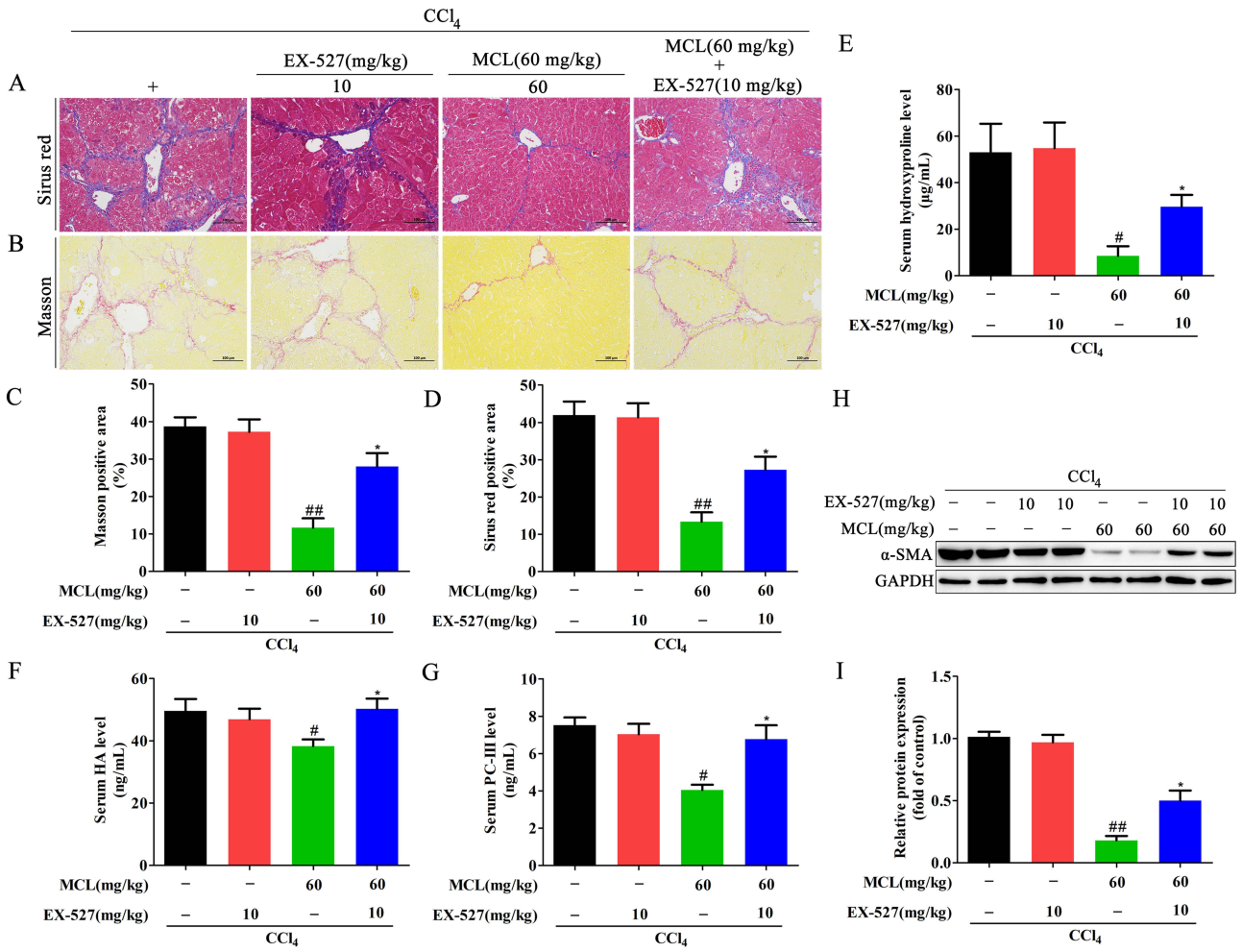

Figure 8 Effect of EX-527 on liver fibrosis regulated by MCL in CCl_4-treated mouse livers. (**A** and **B**) Liver sections were stained with Masson and Sirius red reagents, respectively. Representative photographs are shown (200 × magnification, scale bar: 100 μm). (**C**) Quantified the positive area of Masson staining. (**D**) Quantified the positive area of Sirius red staining. (**E**) Examination of sera levels of hydroxyproline by assay kit in CCl_4-treated mice. (**F** and **G**) Examination of sera levels of HA and PC-III by assay kits in CCl_4-treated mice, respectively. (**H**) Examination of the protein expression of α-SMA by Western blot in CCl_4-treated mouse liver. (**I**) Quantified Western blot results of liver proteins. Data are expressed as mean ± SD (n = 3 of 10 mice). $^{\#}p < 0.05$ and $^{\#\#}p < 0.01$ vs the CCl_4 alone group; $^{*}p < 0.05$ vs the MCL (60 mg/kg) group.

Inhibition of SIRT1 Protein Attenuated the Anti-Inflammatory Effect of MCL Against CCl_4-Induced Liver Inflammation in Mice

To elucidate whether the enhancement of SIRT1 by MCL is directly implicated in its anti-inflammatory effect, we next examined the impact of SIRT1 inhibition on liver inflammation regulated by MCL. Compared to the CCl_4 control group, immunofluorescence analysis revealed that single-agent EX-527 treatment did not significantly affect the expression of IL-6 and IL-1β in mouse liver tissues (Figure 9A and B). In contrast, MCL treatment significantly suppressed the expression of these pro-inflammatory proteins. Conversely, co-treatment of EX-527 markedly alleviated the MCL-mediated inhibition of upregulation of inflammation-associated proteins. In addition, Western blot analysis demonstrated that SIRT1 inhibition attenuated the capacity of MCL to suppress COX-2 protein expression in mouse liver tissues (Figure 9C and D). Furthermore, inhibition of SIRT1 protein also attenuated the capacity of MCL to reduce the serum levels of IL-6 and MCP-1 in mice (Figure 9E and F). Overall, SIRT1 protein inhibition attenuated the anti-inflammatory efficacy of MCL in counteracting CCl_4-induced liver inflammation in mice.

https://doi.org/10.2147/JIR.S559076

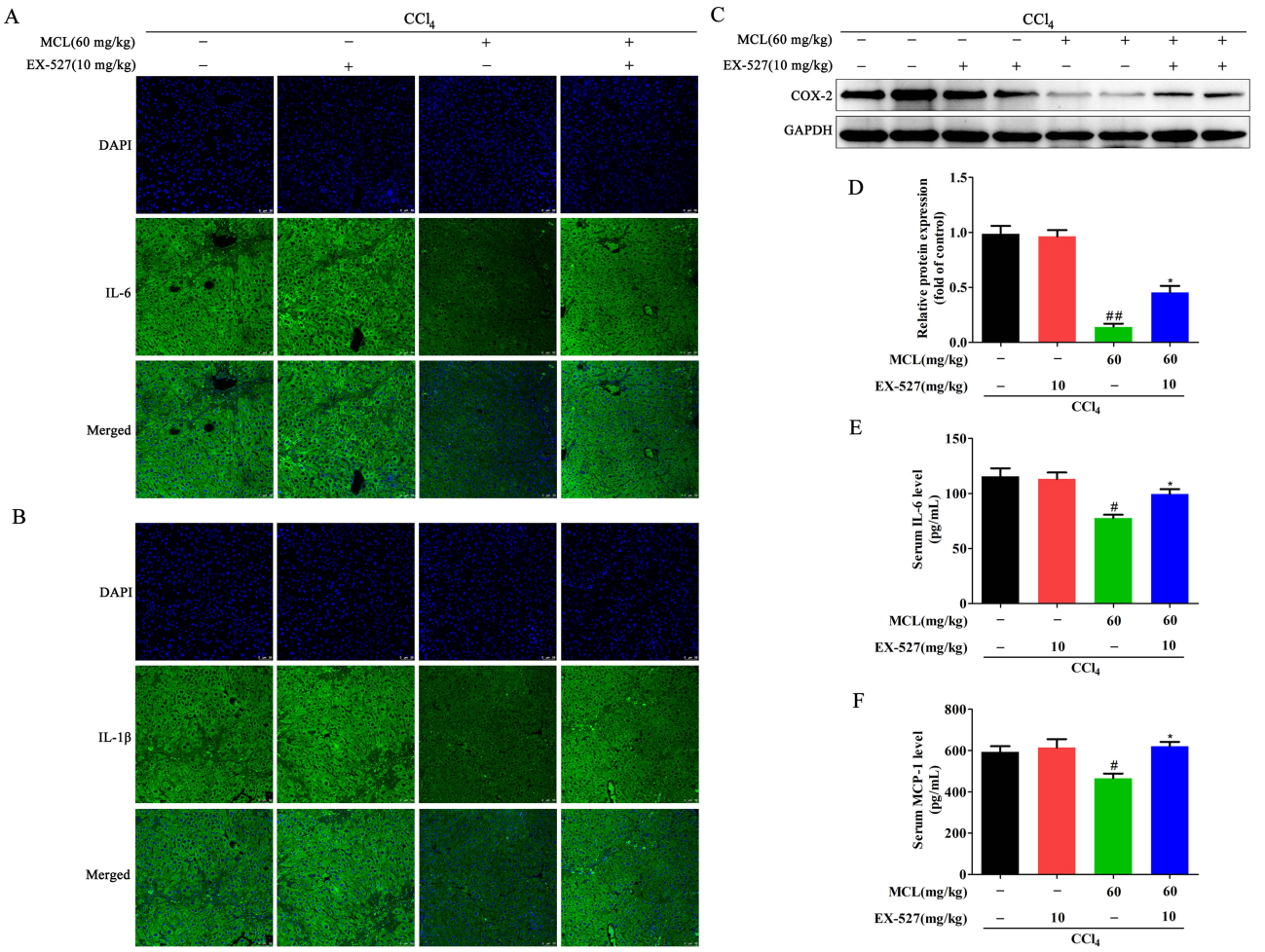

Figure 9 Effect of EX-527 on liver inflammation regulated by MCL in CCl_4-treated mouse livers. (**A**) Immunofluorescence assay was performed to detect the protein expression of IL-6 in mouse liver tissues. (**B**) Immunofluorescence assay was performed to detect the protein expression of IL-1β in mouse liver tissues. (**C**) Examination of the protein expression of COX-2 by Western blot in CCl_4-treated mouse liver. (**D**) Quantified Western blot results of liver proteins. (**E** and **F**) Examination of sera levels of IL-6 and MCP-1 by assay kits in CCl_4-treated mice, respectively. Data are expressed as mean ± SD (n = 3 of 10 mice). $^{\#}p < 0.05$ and $^{\#\#}p < 0.01$ vs the CCl_4 alone group; $^{*}p < 0.05$ vs the MCL (60 mg/kg) group.

Discussion

In this study, we demonstrated that MCL exerts robust protective effects against CCl_4-induced liver injury and fibrogenesis, accompanied by potent anti-inflammatory activity in the livers of mice. Furthermore, mechanistic investigations identified SIRT1 as a key mediator of MCL's therapeutic actions: pharmacological inhibition of SIRT1 markedly abrogated MCL-mediated suppression of hepatic inflammation, thereby impairing its antifibrotic efficacy. To our knowledge, few studies have evaluated the role of MCL in treating CCl_4-induced liver fibrosis through the suppression of liver inflammation via SIRT1 regulation.

Liver inflammatory responses are accompanied by the occurrence and progression of liver fibrosis.[21] Effectively controlling liver inflammation to improve the inflammatory microenvironment around liver tissues represents an effective strategy for alleviating the progression of liver fibrosis.[22] MCL exhibits potent anti-inflammatory activity and can suppress inflammatory responses in multiple pathological contexts, which has established it as a promising inflammatory inhibitor.[23,24] One study reported that MCL effectively alleviated lipopolysaccharide (LPS)-induced severe acute pancreatitis (SAP) mainly by inhibiting pancreatic tissue inflammation in mice. Mechanistically, the anti-inflammatory effect of MCL was partially attributed to the inhibition of nuclear factor kappa B p65 (NF-κB p65).[24] Liu et al found that MCL alleviated diabetic nephropathy by inhibiting the activation of NF-κB signaling in renal tissues, thereby suppressing downstream inflammatory cytokines such as MCP-1, IL-1β, TNF-α, and IL-6.[23] In addition, in an Alzheimer's disease

(AD) mouse model, MCL significantly ameliorated cognitive impairment and exerted a potent anti-neuroinflammatory effect, evidenced by decreased inflammatory cell infiltration, reduced secretion of multiple inflammatory cytokines, and downregulated expression of IL-1β, TNF-α, cyclooxygenase-2 (COX-2), inducible nitric oxide synthase (iNOS) and phosphorylated IκB p65.[25] In the present study, MCL effectively reduced the levels of pro-inflammatory factors and increased the levels of anti-inflammatory factors in the serum of mice. Furthermore, MCL significantly suppressed IL-1β protein expression in liver tissues, thereby demonstrating potent anti-inflammatory activity, which is in line with the findings of previous studies.

Numerous studies have demonstrated that MCL exerts remarkable hepatoprotective effects, with significant inhibitory or alleviating impacts on a wide range of liver-related diseases. In db/db mouse model, MCL was found effectively reduced liver lipid accumulation, thereby alleviating hepatic steatosis.[14] Besides, studies have demonstrated that MCL exerted a potent anti-hepatocellular carcinoma (HCC) effect, effectively suppressing the in vivo growth of HCC. The mechanisms underlying its anti-HCC activity primarily involve inducing apoptosis in HCC cells, disrupting the actin cytoskeleton,[26] and regulating ROS-mediated endoplasmic reticulum stress.[15] Interestingly, the latest findings have revealed that MCL effectively exerts its anti-liver fibrosis activity, and further investigated its potential action mechanisms against liver fibrosis from the perspectives of autophagy regulation and modulation of the ROS/MEK/ERK signaling pathway.[16] In this study, we further revealed that MCL exerted significant anti-liver fibrosis effects, with its mechanism of action elucidated through the regulation of SIRT1-mediated liver inflammation. Thus, our study, in line with prior studies, confirms that MCL demonstrates notable hepatoprotective effects.

Accumulating evidence has confirmed that SIRT1 protein is implicated in the regulatory process of liver fibrosis and has been recognized as an effective therapeutic target for fibrotic liver disease.[27,28] Studies have revealed that SIRT1 protein expression is downregulated in the context of fibrotic liver pathology, whereas activation or upregulation of SIRT1 significantly ameliorates liver fibrosis.[29] Hassan et al found that Dapagliflozin alleviated the bile duct ligation (BDL)-induced liver fibrosis mainly by enhancing SIRT1 expression in liver tissues of rats.[30] Li et al reported that resveratrol alleviated liver fibrosis induced by inorganic mercury exposure by activating the SIRT1/PGC-1α signaling pathway,[20] highlighting the pivotal role of SIRT1 in modulating liver fibrosis. In the present study, we confirmed that MCL significantly increased SIRT1 protein expression in mouse liver tissues through multiple analytical approaches, indicating that SIRT1 upregulation was associated with the process by which MCL alleviated liver fibrosis. To elucidate the role of SIRT1 in this process, we employed the selective SIRT1 inhibitor EX-527 and demonstrated that SIRT1 inhibition potently blunted MCL-mediated anti-liver inflammation, consequently diminishing its anti-fibrotic efficacy. In subsequent investigations, we intend to generate SIRT1 knockout mice to elucidate the impact of SIRT1 ablation on the anti-inflammatory and anti-fibrotic activities of MCL in counteracting CCl_4-induced liver fibrosis in mice. Additionally, the primary limitations of this study are as follows: (1) It is confined to whole-organism level investigations, lacking cellular-level mechanistic studies. (2) The underlying mechanism through which MCL upregulates SIRT1 protein expression remains undefined, requiring further experimental validation to determine whether it is through direct binding or indirect regulation.

Conclusion

In summary, MCL ameliorates CCl_4-induced liver fibrosis in mice by suppressing hepatic inflammation through the upregulation of SIRT1 expression. While additional research is needed to fully elucidate the underlying mechanisms of MCL's protective effects against CCl_4-induced liver fibrosis, our findings suggest that MCL represents a promising candidate for combating liver fibrosis and warrants further preclinical investigation.

Abbreviations

α-SMA, α-smooth muscle actin; ALP, alkaline phosphatase; ALT, alanine aminotransferase; AST, aspartate aminotransferase; BDL, bile duct ligation; CCl_4, carbon tetrachloride; COX-2, cyclooxygenase-2; ECM, extracellular matrix; HA, hyaluronic acid; HSCs, hepatic stellate cells; IL-1β, interleukin-1β; iNOS, inducible nitric oxide synthase; LDH, lactic dehydrogenase; LN, laminin; LPS, lipopolysaccharide; MCL, Micheliolide; MCP-1, monocyte chemoattractant protein-1; PC-III, Procollagen Type III; SIRT1, Sirtuin 1; SIR2, silent information regulator 2; TNF-α, tumor necrosis factor-α.

Data Sharing Statement

All data and materials are available from the corresponding author upon request.

Funding

The present study was supported by the grants from the National Natural Science Foundation of China (82374228, 82274339).

Disclosure

The authors declare that there are no competing interests in this work.

References

1. Zhang W, Wu W, Zhang N, et al. Hepatic stellate cell-derived microfibrillar-associated protein 2 prevents liver fibrosis by regulating extracellular matrix and inflammation. *Theranostics*. 2025;15(9):4033–4053. doi:10.7150/thno.109771
2. Zhang L, Lin W, Cai Y, et al. Farnesoid X receptor activation is required for the anti-inflammatory and anti-oxidative stress effects of Alisol B 23-acetate in carbon tetrachloride-induced liver fibrosis in mice. *Int Immunopharmacol*. 2023;123:110768. doi:10.1016/j.intimp.2023.110768
3. Sun HM, Feng QY, Qin BF, et al. Bruceine A attenuates fibrogenesis and inflammation through NR2F2-regulated HMGB1 inflammatory signaling cascades in hepatic fibrosis. *Eur J Pharmacol*. 2025;987:77164. doi:10.1016/j.ejphar.2024.177164
4. Zhang L, Zhang H, Gu J, et al. Glabridin inhibits liver fibrosis and hepatic stellate cells activation through suppression of inflammation and oxidative stress by activating PPARgamma in carbon tetrachloride-treated mice. *Int Immunopharmacol*. 2022;113(Pt B):109433. doi:10.1016/j.intimp.2022.109433
5. Wang P, Wang R, Zhao W, et al. Gut microbiota-derived 4-hydroxyphenylacetic acid from resveratrol supplementation prevents obesity through SIRT1 signaling activation. *Gut Microbes*. 2025;17(1):2446391. doi:10.1080/19490976.2024.2446391
6. Xu M, Zhao Y, Gong M, et al. Dehydroevodiamine ameliorates neurological dysfunction after traumatic brain injury in mice via regulating the SIRT1/FOXO3a/Bim pathway. *Phytomedicine*. 2024;125:155321. doi:10.1016/j.phymed.2023.155321
7. Wang J, Wu R, Hua Y, et al. Naringenin ameliorates vascular senescence and atherosclerosis involving SIRT1 activation. *J Pharm Pharmacol*. 2023;75(8):1021–1033. doi:10.1093/jpp/rgad053
8. Tian L, Chen J, Yang M, et al. Xiezhuo Tiaozhi formula inhibits macrophage pyroptosis in the non-alcoholic fatty liver disease by targeting the SIRT1 pathway. *Phytomedicine*. 2024;131:155776. doi:10.1016/j.phymed.2024.155776
9. Xia Y, Luo Q, Gao Q, et al. SIRT1 activation ameliorates rhesus monkey liver fibrosis by inhibiting the TGF-beta/smad signaling pathway. *Chem Biol Interact*. 2024;394:110979. doi:10.1016/j.cbi.2024.110979
10. He S, Wang Y, Liu J, et al. Activating SIRT1 deacetylates NF-kappaB p65 to alleviate liver inflammation and fibrosis via inhibiting NLRP3 pathway in macrophages. *Int J Med Sci*. 2023;20(4):505–519. doi:10.7150/ijms.77955
11. Guo JS, Wang JY, Chen SH, et al. The natural product micheliolide promotes the nuclear translocation of GAPDH via binding to Cys247 and induces glioblastoma cell death in combination with temozolomide. *Biochem Pharmacol*. 2025;233:116759. doi:10.1016/j.bcp.2025.116759
12. Gan Z, Huang J, Xu M, et al. Micheliolide prevents estrogen deficiency-induced bone loss via inhibiting osteoclast bone resorption. *Aging*. 2023;15(19):10732–10745. doi:10.18632/aging.205111
13. Li W, Li Y, Xiao L, et al. Micheliolide attenuates sepsis-induced acute lung injury by suppressing mitochondrial oxidative stress and PFKFB3-driven glycolysis. *J Transl Med*. 2025;23(1):181. doi:10.1186/s12967-024-05906-0
14. Zhong J, Gong W, Chen J, et al. Micheliolide alleviates hepatic steatosis in db/db mice by inhibiting inflammation and promoting autophagy via PPAR-gamma-mediated NF-B and AMPK/mTOR signaling. *Int Immunopharmacol*. 2018;59:197–208. doi:10.1016/j.intimp.2018.03.036
15. Xu Z, Xu J, Sun S, et al. Mecheliolide elicits ROS-mediated ERS driven immunogenic cell death in hepatocellular carcinoma. *Redox Biol*. 2022;54:102351. doi:10.1016/j.redox.2022.102351
16. Liu Y, Yao L, Liu Y, et al. Micheliolide alleviates hepatic fibrosis by inhibiting autophagy in hepatic stellate cells via the TrxR1/2-mediated ROS/MEK/ERK pathway. *Pharmaceuticals*. 2025;18(3):287. doi:10.3390/h18030287
17. Zhao S, Li J, Xing X, et al. Oxyberberine suppressed the carbon tetrachloride-induced liver fibrosis by inhibiting liver inflammation in a sirtuin 3-dependent manner in mice. *Int Immunopharmacol*. 2023;116:109876. doi:10.1016/j.intimp.2023.109876
18. Liang CL, Wei YY, Chen Y, et al. Zhen-Wu-Tang ameliorates lupus nephritis by diminishing renal tissue-resident memory CD8(+) T cells via suppressing IL-15/STAT3 pathway. *Biomed Pharmacother*. 2024;174:116597. doi:10.1016/j.biopha.2024.116597
19. Lv T, Fan X, He C, et al. SLC7A11-ROS/alphaKG-AMPK axis regulates liver inflammation through mitophagy and impairs liver fibrosis and NASH progression. *Redox Biol*. 2024;72:103159. doi:10.1016/.redox.2024.103159
20. Li S, Han B, Li J, et al. Resveratrol alleviates liver fibrosis induced by long-term inorganic mercury exposure through activating the Sirt1/PGC-1alpha signaling pathway. *J Agric Food Chem*. 2024;72(28):15985–15997. doi:10.1021/acs.jafc.4c02349
21. Chen C, Gu J, Wang J, et al. Physcion 8-O-beta-glucopyranoside ameliorates liver fibrosis through inflammation inhibition by regulating SIRT3-mediated NF-kappa B P65 nuclear expression. *Int Immunopharmacol*. 2021;90:107206. doi:10.1016/j.intimp.2020.107206
22. Zhang JJ, Zhang JX, Feng QY, et al. Eriocitrin ameliorates hepatic fibrosis and inflammation: the involvement of PPARalpha-mediated NLRP1/NLRC4 inflammasome signaling cascades. *J Ethnopharmacol*. 2025;338(Pt 3):119119. doi:10.1016/j.jep.2024.119119
23. Liu W, Chen X, Wang Y, et al. Micheliolide ameliorates diabetic kidney disease by inhibiting Mtdh-mediated renal inflammation in type 2 diabetic db/db mice. *Pharmacol Res*. 2019;150:104506. doi:10.1016/phrs.2019.104506
24. Wu CY, Wang KQ, Qin YY, et al. Micheliolide ameliorates severe acute pancreatitis in mice through potentiating Nrf2-mediated anti-inflammation and anti-oxidation effects. *Int Immunopharmacol*. 2024;143(Pt 2):113490. doi:10.1016/j.intimp.2024.113490
25. Yang G, Hu Y, Qin X, et al. Micheliolide attenuates neuroinflammation to improve cognitive impairment of Alzheimer's disease by inhibiting NF-kappaB and PI3K/Akt signaling pathways. *Heliyon*. 2023;9(7):e17848. doi:10.1016/j.heliyon.2023.e17848

26. Yu L, Chen W, Tang Q, et al. Micheliolide inhibits liver cancer cell growth via inducing apoptosis and perturbing actin cytoskeleton. *Cancer Manag Res*. 2019;11:9203–9212. doi:10.2147/CMAR.S216870
27. Liu J, Ma X, Guo W, et al. Deacetylation of HnRNP U mediated by sirtuin1 ameliorates aged rat with liver fibrosis via inhibiting p53-related senescence and NLRP3-related inflammation. *Int Immunopharmacol*. 2024;141:113026. doi:10.1016/j.intimp.2024.113026
28. Adjei-Mosi J, Sun Q, Smithson SB, et al. Age-dependent loss of hepatic SIRT1 enhances NLRP3 inflammasome signaling and impairs capacity for liver fibrosis resolution. *Aging Cell*. 2023;22(5):e13811. doi:10.1111/acel.13811
29. Qin T, Hasnat M, Wang Z, et al. Geniposide alleviated bile acid-associated NLRP3 inflammasome activation by regulating SIRT1/FXR signaling in bile duct ligation-induced liver fibrosis. *Phytomedicine*. 2024;129:155405. doi:10.1016/j.phymed.2024.155405
30. Hassan HA, Nageeb MM, Mohammed HO, et al. Dapagliflozin dampens liver fibrosis induced by common bile duct ligation in rats associated with the augmentation of the hepatic Sirt1/AMPK/PGC1alpha/FoxO1 axis. *Toxicol Appl Pharmacol*. 2024;489:116991. doi:10.1016/j.taap.2024.116991